DISTRIBUTION STATEMENT A. Approved for public release; distribution is unlimited.

DARLA: Data Assimilation and Remote Sensing for Littoral Applications

Andrew T. Jessup
Chris Chickadel, Gordon Farquharson, Jim Thomson
Applied Physics Laboratory, University of Washington
Seattle, WA 98105
phone: ((206) 685-2609 fax: (206) 543-6785 email: jessup@apl.washington.edu

Robert A. Holman
Merrick Haller, Alexander Kuropov, Tuba Ozkan-Haller
Oregon State University
Corvallis, OR 97331
phone: (541) 737-2914 fax: (541) 737-2064 email: holman@coas.oregonstate.edu

Steve Elgar
Britt Raubenheimer
Woods Hole Oceanographic Institution, MS11
Woods Hole, MA 02543
phone: (508) 289-3614 fax: (508) 457-2194 email: elgar@whoi.edu

Award Number: N000141010932

LONG-TERM GOALS

Our long-term goal is to use remote sensing observations to constrain a data assimilation model of wave and circulation dynamics in an area characterized by a river mouth or tidal inlet and surrounding beaches. As a result of this activity, we will improve environmental parameter estimation via remote sensing fusion, determine the success of using remote sensing data to drive DA models, and produce a dynamically consistent representation of the wave, circulation, and bathymetry fields in complex environments.

OBJECTIVES

The objectives are to test the following three hypotheses:

1. Environmental parameter estimation using remote sensing techniques can be significantly improved by fusion of multiple sensor products.
2. Data assimilation models can be adequately constrained (i.e., forced or guided) with environmental parameters derived from remote sensing measurements.
3. Bathymetry on open beaches, river mouths, and at tidal inlets can be inferred from a combination of remotely-sensed parameters and data assimilation models.

APPROACH

Our overall approach is to conduct a series of field experiments combining remote sensing and in situ measurements to investigate signature physics and to gather data for developing and testing DA models. To ensure early and ongoing testing, we performed a pilot experiment at Duck, NC, using tower-based remote sensing (EO, radar, IR) and current versions of the DA modeling system. We participated in the field experiment in May 2012 at New River Inlet near Camp LeJeune, NC under the ONR-sponsored Inlets and Rivers Mouth Dynamics Departmental Research Initiative (RIVET). This approach benefits both the remote sensing research (by leveraging the RIVET in situ measurements) and RIVET itself via our integrated remote sensing and DA modeling system. The combined capabilities provide an innovative solution that couples spatially dense sampling with data assimilation methods to study the complicated dynamics of interacting wave, bathymetry, and current fields. The key to this project is an interactive process that blends sophisticated remote sensing, in-situ sensing, and data assimilation modeling. Our approach is to conduct closely coupled field and numerical model experiments to test the hypotheses listed above. Work on each facet informs the work on the others, and conflicts in results or interpretations are resolved by testing the hypotheses and the sensitivity of the results to a range of parameter variations.

WORK COMPLETED AND RESULTS

During the second year, we participated in the RIVET DRI experiment in May 2012 at New River Inlet, NC. We also worked on analysis and assimilation of the data from the Duck pilot experiment and on coupled wave-circulation models.

Due to the number of investigators involved and the complexity of the project, we have chosen to provide a section for each team which combines their Work Completed and Results contributions. The lettered sections correspond to the following teams:

A. Infrared Remote Sensing – UW: Chickadel and Jessup

B. Electro-Optical Remote Sensing – OSU: Holman

C. Microwave Remote Sensing – UW: Farquharson

D. Microwave Remote Sensing – OSU: Haller

E. In situ Measurements – UW: Thomson

F. In situ Measurements – WHOI: Elgar and Raubenheimer

G. Numerical Modeling and Data Assimilation – OSU: Ozkan-Haller and Kurapov

A. Infrared Remote Sensing – UW

Our work on littoral and estuarine thermal signatures in FY12 has focused on a major field effort at the New River Inlet experiment (NRI) which took place in May 2012. At NRI we deployed three separate systems, plane, tower and a mobile platform, to measure multiple scales during the three-week effort. We first cover the new data from NRI with examples. The goals guiding our experiments and analysis are:

1. Estimating geophysical parameters from surface IR signatures including currents, wave parameters, and wave breaking,
2. Validation of remotely sensed waves and currents with in situ data, and
3. Providing data with confidence limits for inclusion into data assimilation.

New River Inlet

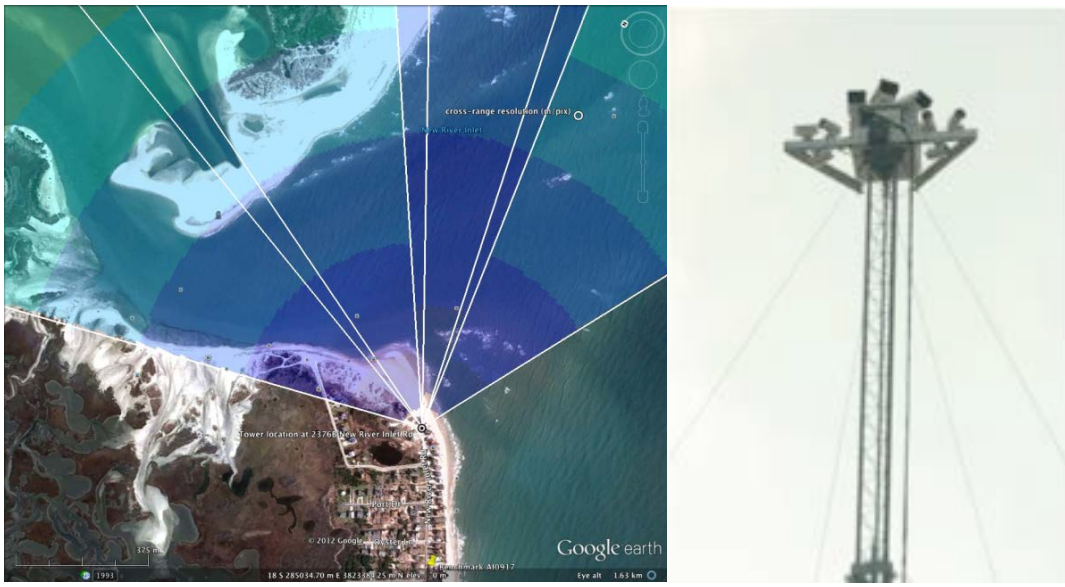

Figure A1. (left) Combined field of view for the APL-UW IR camera tower at the New River Inlet 2012 experiment. (right) Image of the camera arrays on the top of the tower. APL-UW IR cameras are in the square housings on the top of the installation. OSU EO cameras are the smaller barrel housings on the lower armature.

Tower – An array of four uncooled thermal cameras was mounted on a 32 m tower positioned approximately 200 m southeast of the southern edge of the inlet (Figure A1). The cameras viewed about 130° in their overlapping configuration including north into the inlet and out into the inlet mouth. Digital, 14 bit, full frame video was recoded from each camera at 10 Hz, 24 hours a day from 26 April until demobilization on 19 May (24 days). Short, infrequent data gaps (few hours to half a day) were unpreventable due to lowering the tower for approaching electrical storms. Figure A2a, shows an example view fro each of the four cameras displaying cool exposed beaches (dark in the image), bright wave crests and a body of warmer water hugging the shore. Using the surveyed ground targets and camera positions, we are able rectify the imagery to local coordinate systems and in the process stitching the images together in a single mosaic. The mosaic in Figure A2b shows a processed image where we have calculated the mean intensity over five seconds. Using consecutive 5 s image means, which effectively removed the signal of short waves, we were able to successfully estimate the surface velocity patterns of the dominant tidal currents with a particle image velocimetry (PIV) technique which we demonstrate in the Surf Zone Optics experiment in 2010. The complex 100 m-scale flow over the main inlet channel demonstrates large gradients, specifically near the mouth where the channel shoals abruptly and the currents stagnate. We will process the rest of the three weeks of data to investigate tidal patterns of the currents here and plan to integrate the results with in situ measurements to verify and guide models.

a

b

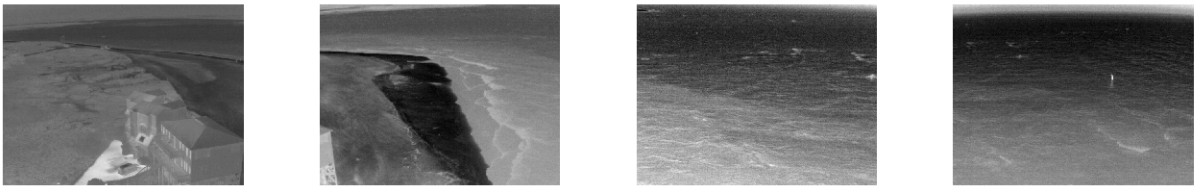

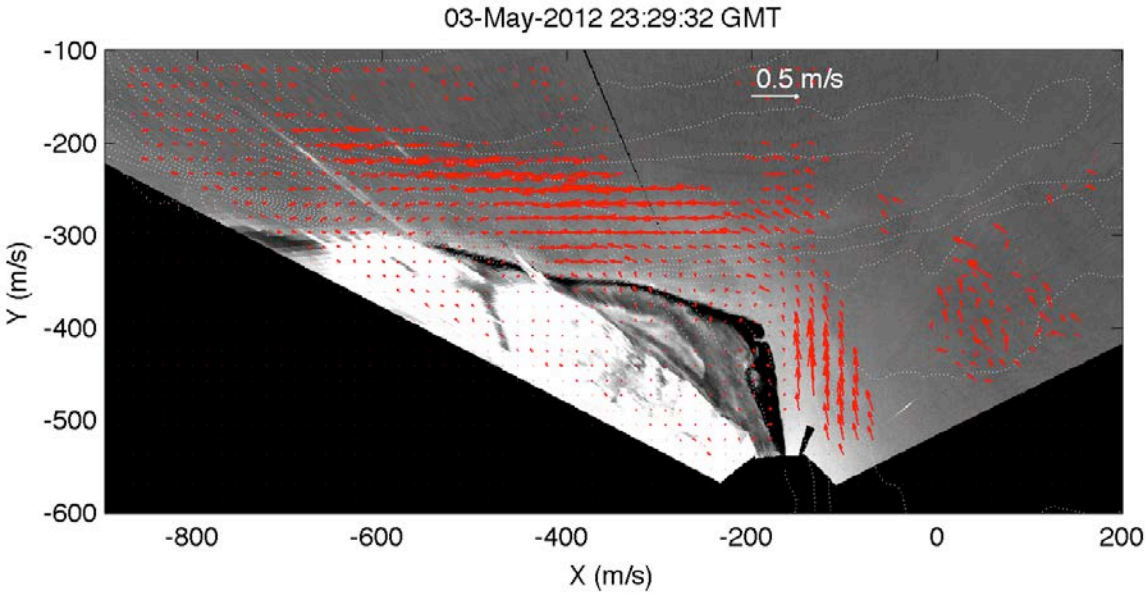

Figure A2. (a) the four independent IR camera views of the New River Inlet from up inlet (left) to offshore (right). Note the warmer (brighter) water hugging the shore on these flood tide images (b) A rectified five-second time averaged mosaic of all four cameras. Red vectors show the PIV calculated surface velocity over the main inlet channel and indicate a stagnation point at y = -200, x = -300.

Plane – A two-camera thermal imaging system mounted on a Cessna 172 was deployed regularly throughout the NRI experiment. This imaging system was adjoined to a microASAR (operated and analyzed by G. Farquharson) to provide thermal imagery simultaneous and spatially coincident with the microASAR collections. Details of deployment times and transect locations are described in the section on airborne radar, however transects were taken approximately twice every three days for 3-4 hours at a time and transects parallel and perpendicular to the coast in the vicinity of the inlet were flown. The system includes a high accuracy Inertial Navigation System ($O(0.01)$ rms error on attitude) which enables accurate georectification. Figure A3 displays a rectified image from the airborne IR system and demonstrates the observed temperature signals in the offshore plume that emanates from the inlet on ebb tides. The plume is a complex set of multiple fronts with 200 m – 400 m spacings that rim the southern boundary of the plume. The surface temperature differences observed in the plume are of order 1 °C. As we continue to map more of the plumes from different stages of the tide during the experiment we are developing algorithms to correct for thermal drift that occurs with uncooled thermal cameras, which causes the blocky pattern in the mosaic in Figure A3.

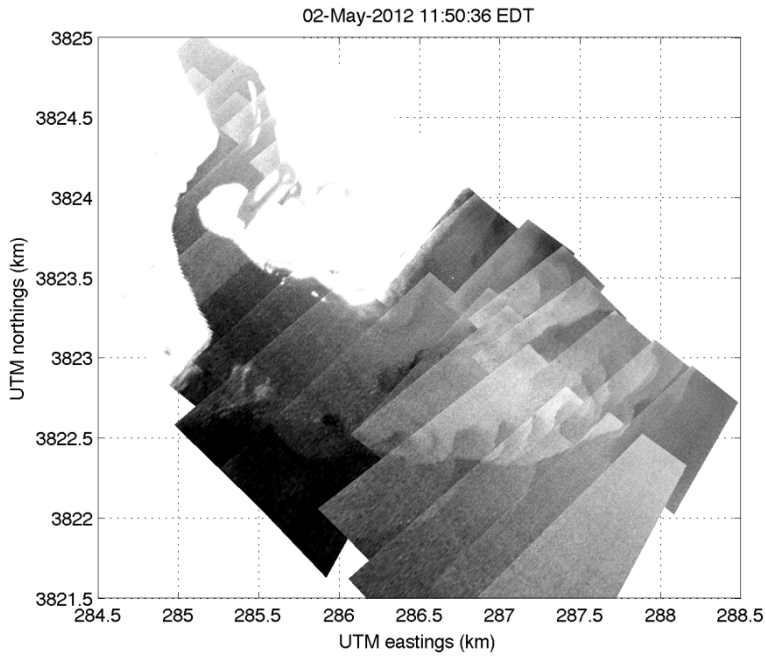

Figure A3. A georectified thermal image from the airborne IR system of the APL-UW Cessna. A relatively warmer plume is identifiable exiting from the New River inlet on an ebb tide early in the experiment. The plume is driting north and multiple complex frontal features are observed on its southern boundary.

Mobile (LTAIRS) system – Our third IR imaging system is the Lighter-Than-Air Infrared System (LTAIRS) that was deployed early in the NRI experiment, however stronger than expected winds prevented us from safely flying the balloon for the rest of the experiment. Instead we took advantage of convenient, low-altitude, fixed locations to mount the LTAIRS cameras and data recorder, to achieve high-resolution thermal imaging of both surface inlet flow and surf zone wave breaking and currents. We were able to sample for approximately six days total, and our preliminary data review is only just beginning as we focus on airborne and tower data.

B. Electro-Optical Remote Sensing - OSU

The goal of the electro-optical component of DARLA is to develop and test algorithms for estimating relevant geophysical variables based on optical data, to work with modelers who will be developing methods to assimilate these data using appropriate statistical methods of data assimilation, and to compare data to synchronous results from companion radar and infrared sensors to search for new opportunities in data fusion. A major effort for FY12 was preparation for, participation in, and analysis of data from the May, 2012 New River Inlet field experiment. This field campaign extended our traditional sampling experience to a tidal inlet where the effects of waves, bathymetry and currents all co-mingle in variable but roughly equal amounts.

The experiment took place over a three-week period and featured fixed-base optical remote sensing using Argus cameras mounted on a 32 m high elevating tower arranged by UW-APL. Six cameras allowed optical coverage over roughly 200 degrees of azimuth from the open beach to the south to part

way up the tidal inlet (Figure B1). Time series and image data were collected every 30 minutes of daylight, analyzed on site and placed on a common ftp site in MATLAB format for common use.

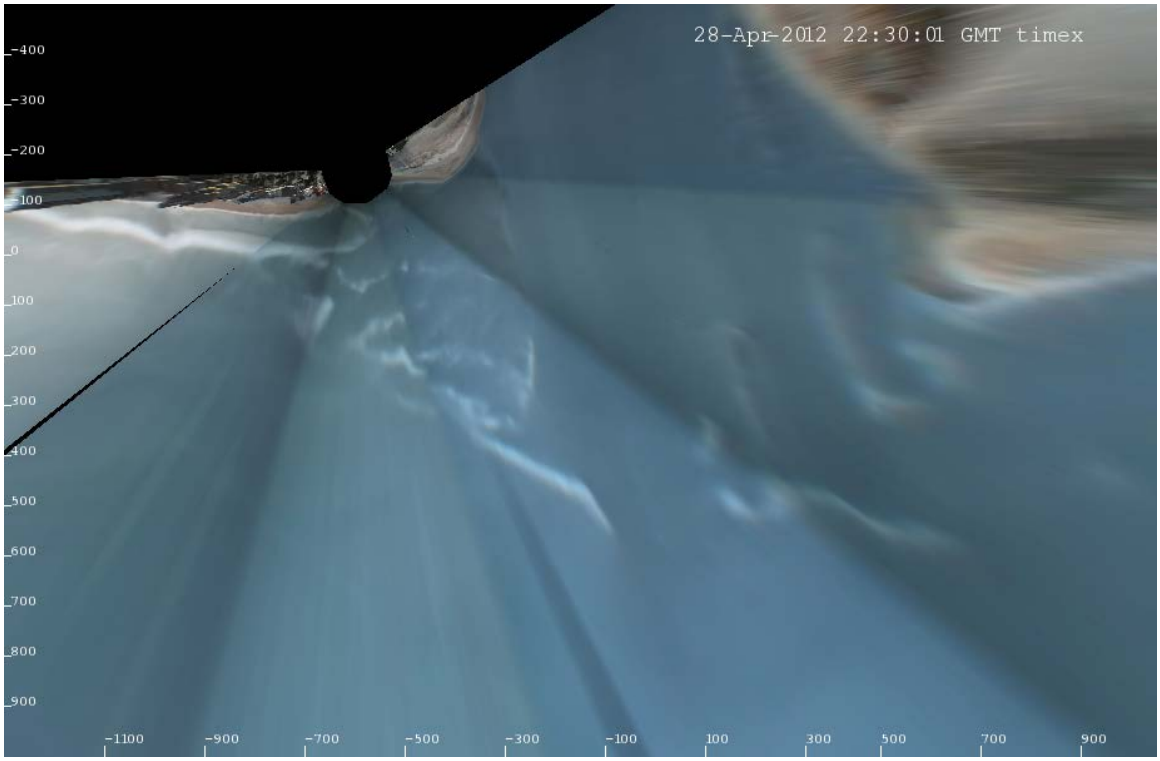

Figure B1. Example rectified time exposure image from the RIVET field experiment, May, 2012. Shadow-like "spokes" in the image correspond to the boundaries between the six cameras which were located on a mast at the nub in the black (unsampled) area. White features correspond to wave breaking over submerged shoal and indicated the complexity of the delta morphology.

In addition, we have continued analysis of data from the previous Surf Zone Optics experiment from September, 2010 with the main focus on final testing of the cBathy algorithm, development of optical wave dissipation algorithms and automated current estimation for integration into the data assimilation machinery.

The primary accomplishment has been the completion and publication of the cBathy algorithm (Holman et al, in review). This paper demonstrated that the algorithm provides accurate (0.19 m bias, 0.51 m rmse error) bathymetry estimates over a large region (1000 x 500 m) using only turn-key settings and production analysis with no pre-qualification on the ingested data (for an example result, Figure B2). This algorithm is now being run at numerous Argus sites around the world and should provide a solid enduring bathymetry capability at low cost. cBathy also returns map estimates of wave frequency and direction over time. Efforts are underway to assimilate these basic variables into nearshore numerical models.

The second main accomplishment is the successful completion of the New River Inlet field experiment. The study region was large, complex and logistically disadvantaged so the challenges

were many and expectations mixed. However, the fixed-platform EO sampling of Argus worked surprisingly well and has already revealed unexpected patterns in the mobility and migration of complex ebb tidal shoals and a promising capability in bathymetry and current estimation (that needs continuing investigation).

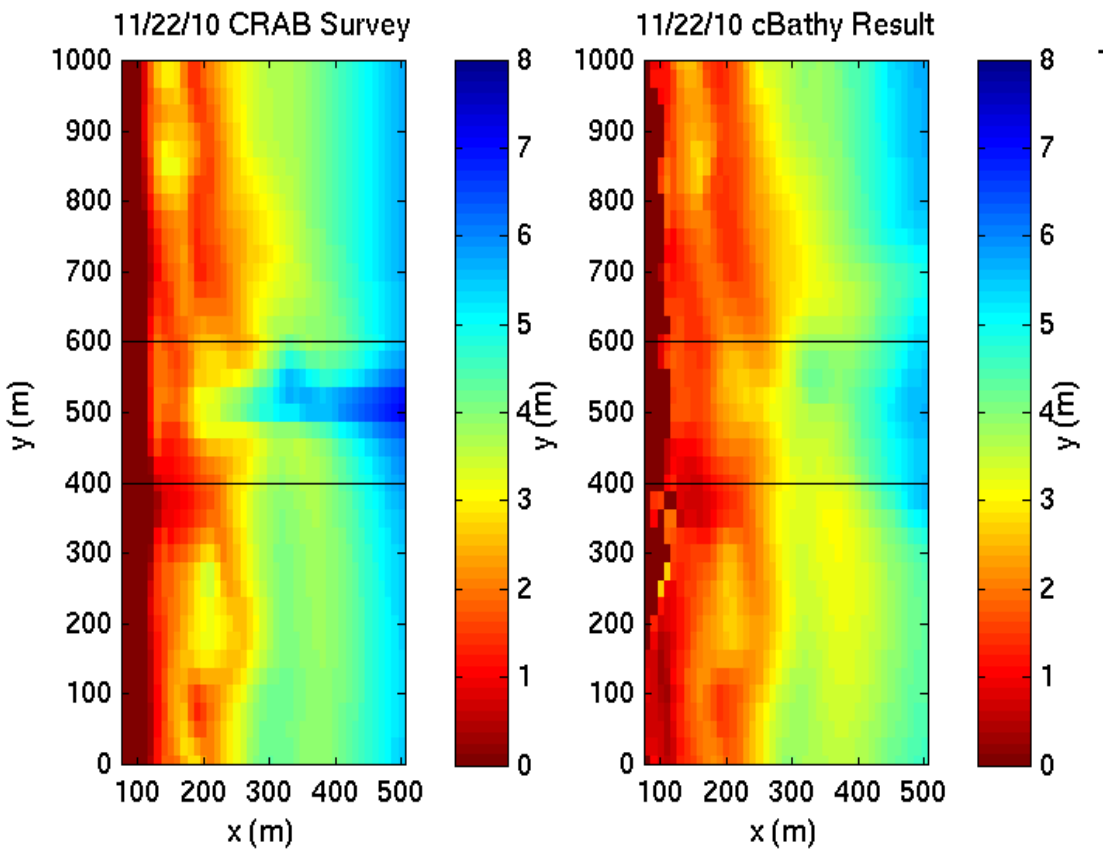

Figure B2. Ground truth bathymetry data (left) and cBathy estimates (right) computed solely from optical observations for an example survey on 11/22/10. The region between the two black lines corresponds to a pier near which both in situ and optical data are obscured. Excluding these regions, the bias and rmse error between the two was 0.19 and 0.51 m, respectively. It was surprising how well details in the sand bar are reproduced.

We now have a robust capability to measure nearshore bathymetry through variable and non-optimal conditions. The algorithm also returns important data on the frequencies and directions of the nearshore wave field along with the confidence limits needed to integrate these data into data assimilative tools or other downstream products. We have found (but not yet published) that ebb delta shoals display a surprising and organized mobility and migration pattern.

C. Microwave Remote Sensing – UW

Dual-beam ATI microASAR

Installation of the dual-beam along-track interferometric microASAR on the aircraft started early in 2012 (Figure C1). FAA approval for the antenna platform was obtained in February, and the first test flights for radar were conducted on March 8 and March 23. Deception Pass and Skagit Bay in Washington State were chosen for these test flights because of the strong tidally-driven flow through the pass and the tidal deltas in the Skagit Bay area. Based on these tests, we made small modifications to the installation to improve the performance and accuracy. We verified the operation of the system by forming synthetic aperture images for the forward-squinted and the aft-squinted radars.

Figure C1: microASAR antennas and IR/visible cameras installed on the belly of the Cessna 172.

The system was deployed at the New River Inlet in North Carolina from April 30 to May 21. We conducted 16 flights (Table C1). Flight times were chosen to coincide with phases of the tide and measurement conditions (wind, clouds, etc.) and other project-related events (SWIFT measurements, other airborne measurements, dye releases, and satellite overpasses). Measurements during each flight were limited to around 2.5 hours because the ferry time from the airport to the site was around 30 minutes each way.

Table C1: Aircraft approximate measurement times. All times are in EDT (UTC-4).

Date	Start	End	Tide	
2012-04-30	17:20	17:51		
2012-05-01	14:54	16:37	High at 16:14	Before high (1)
2012-05-02	10:08	12:28	Low at 10:49	After low (1)
2012-05-04	09:15	10:45	Low at 12:29	Before low (1)
2012-05-06	17:22	19:54	High at 20:42	Before high (2)
2012-05-07	09:53	11:48	High at 09:03	After high (1)
2012-05-08	12:29	14:59	Low at 15:55	Before low (2)
2012-05-10	17:58	20:25	Low at 17:51	After low (2)
2012-05-11	08:15	10:47	Low at 06:54	After low (3)
2012-05-13	12:09	14:57	High at 15:05	Before high (3)
2012-05-17	13:12	14:13	Low at 11:58	After low (4)
2012-05-18	10:55	12:50	Low at 12:36	After low (5)
2012-05-19	06:56	09:26	High at 07:20	After high (3)
	13:31	14:17		
2012-05-20	10:33	12:59	Low at 13:48	Before low (3)
2012-05-21	05:44	08:24	High at 20:57	Before high (4)

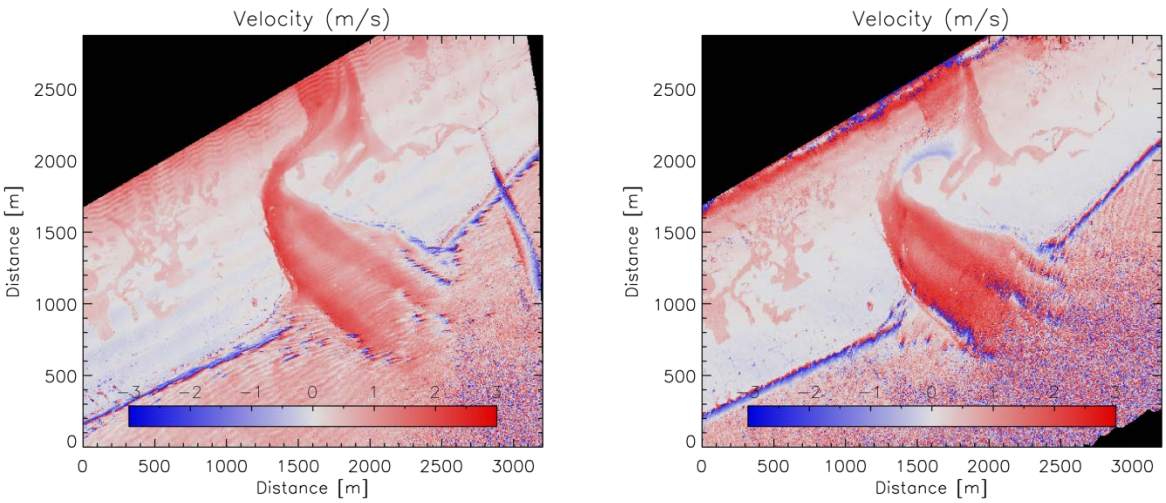

Figure C2: Estimates of surface velocity from the aft- (left) and forward-squinted (right) radars during an ebb tide on May 10 2012 at 17:58 EDT (21:58 UTC). The wind speed was around 5.5 m/s, and the wind direction was 334°T.

We have developed code to form interferograms from each of the squinted-SAR systems, and have estimated the radial components of the surface velocity (Figure C2). These radial components are combined to form a vector velocity field (Figure C3), but the accuracy of these vectors will be improved by updating the SAR processing code to deal with various artifacts of our particular measurement.

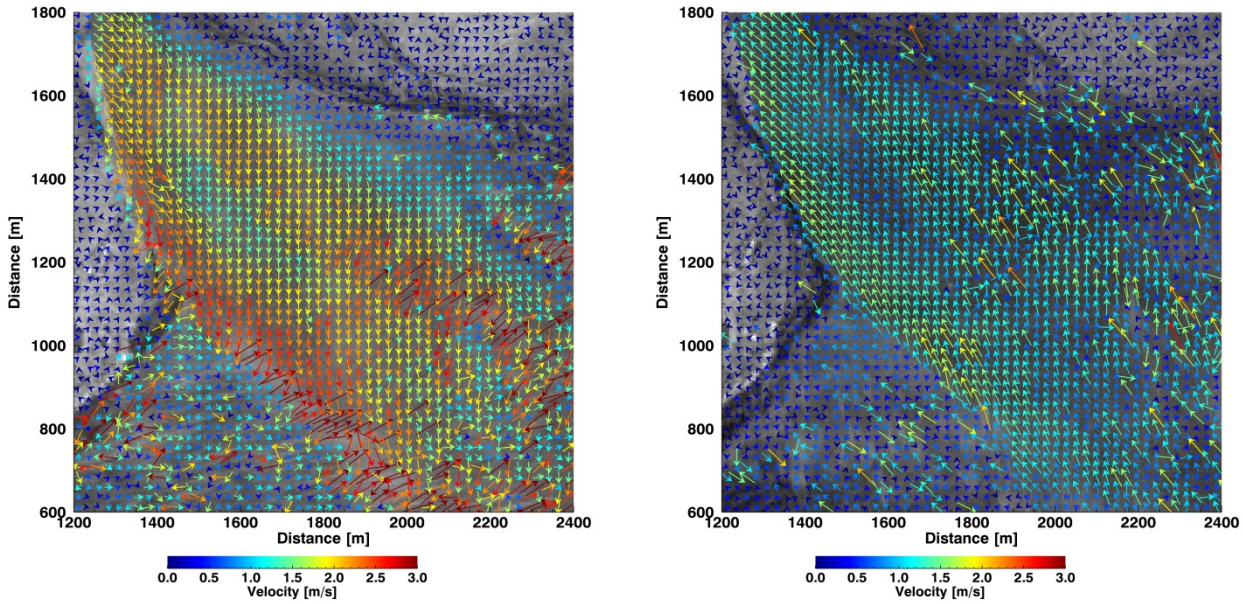

Figure C3: Surface velocities estimated from the interferometric SAR measurements during an ebb tide (left) and a flood tide (right).

We are working on several upgrades to the SAR processing code developed by Artemis, which will allow us to create more accurate surface vector velocity maps. Currently, our SAR processing code does not account for the azimuthal subsampling scheme implemented in the radar. As a result, the forward- and aft-squinted images are azimuthally offset from one another. We also have a small range dependent interferometric phase ripple (visible in the aft-squinted image in Figure C2) that we need to characterize and remove. We also need to study various methods for converting interferometic phase to surface velocity for the time-domain back projection SAR processing code that we are using to process the SAR data, to characterize retrieval errors, and thereby eliminate poor velocity estimates so that the fields can be assimilated into the models.

Photographs (Figure C4) of the inlet were taken during all flights with a hand-held camera. We have posted these photographs to a publicly available site (http://apluwrivetphotos.shutterfly.com/pictures) for general use.

Figure C4: Photographs taken of the New River Inlet on May 1, May 2, and May 10. The photographs show the large changes in wave breaking around the inlet at different times of the tidal cycle and the complex refraction of waves (right-hand photograph). The middle picture highlights the extensive ebb-tide plume that existed at times during the experiment.

CORAR

We installed the Coherent Real Aperture Radar (CORAR) on top of scaffolding next to the New River Inlet (Figure C3). CORAR was operational from May 10 to May 22 (13 days). The system collected data continuously, with only a brief interruption around noon each day to service the generator.

Figure C3: CORAR was deployed on the south bank of the inlet (34.529695, -77.344419). The antennas were on top of scaffolding at a height of around 12 m above the water.

The radar was configured to measure mean surface currents by staring in a particular direction for several seconds. In this mode, the wave field is blurred, but measurement of the Doppler spectrum in each range cell is possible. The radar was programmed to produce a scan over the inlet approximately every 15 minutes. The radar recorded backscattered power and Doppler shift (Figure C4).

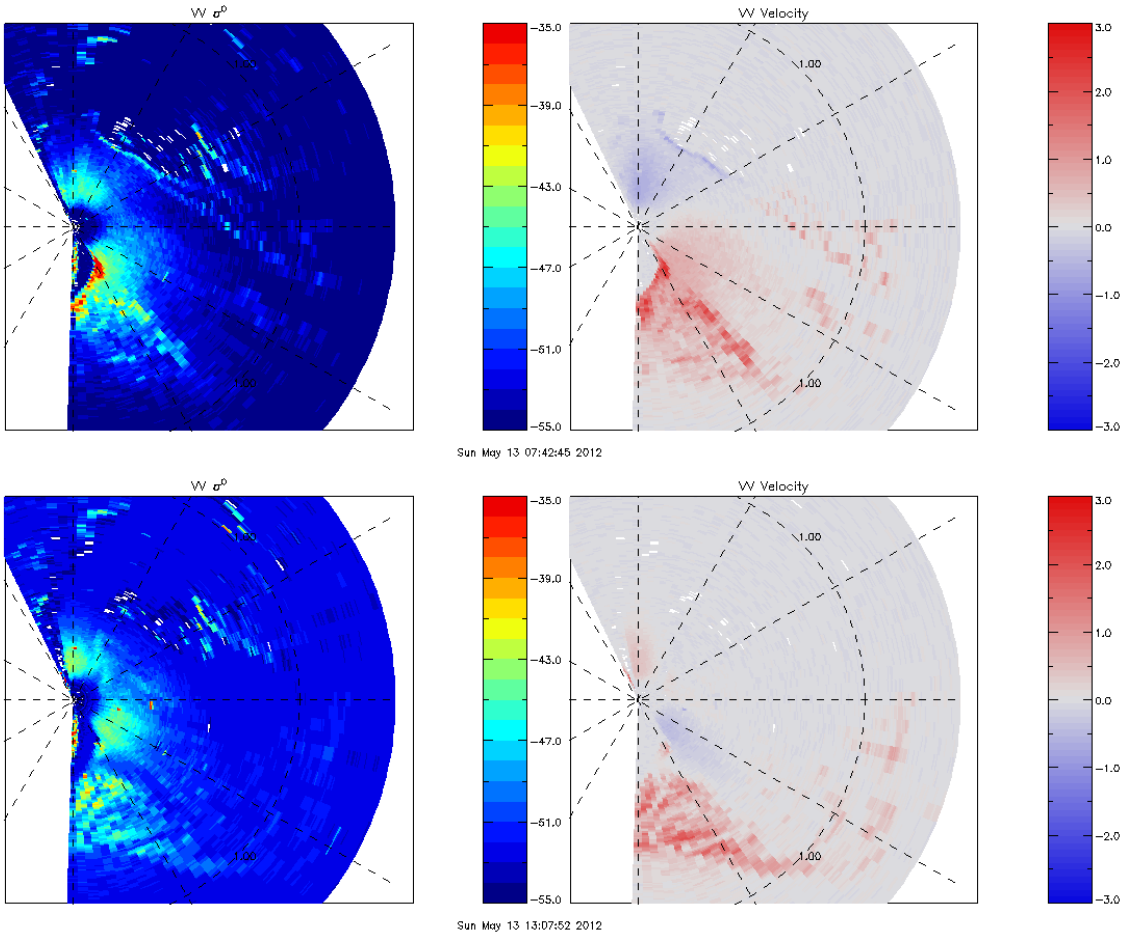

Figure C4: CORAR backscattered power image (left) and Doppler velocity image (right) recorded on May 13 at 03:42 EDT (07:42 UTC) (top) and 09:07 EDT (13:07 UTC) (bottom). The Doppler velocity shows the reversal in the flow in the inlet. High tide was 02:20 EDT (05:20 UTC) and low tide was 08:49 EDT (12:49 UTC). One can also see the difference in position between the zones of breaking waves.

We are working on quality control of the data. We plan to compare the CORAR data with the microASAR surface velocity measurements, the Oregon State University Doppler radar measurements, and IR and visible camera derived surface currents, and near surface in situ measurements (e.g., SWIFTs). If there is sufficient overlap between the microwave radars, we will attempt dual-Doppler processing to retrieve surface currents within and around the inlet.

Microwave Remote Sensing – OSU

DARLA-MURI FY2012

- Hired Postdoctoral Scholar (Guillermo Mendez Diaz) November, 2011.
- Analysis of the rip currents imaged at Duck during pilot experiment is nearly complete. Importance of alongshore wind stress on the rip current flow field and cross-shore wind stress on the rip current imaging has been quantified. Results are being submitted this fall (Haller, M.C. et al., Radar remote sensing of rip currents, in preparation for *Geophysical Research Letters*, 2012).
- Participated in RIVET field experiment, April-May 2012, collected marine radar observations (WIMR in both incoherent and coherent-on-receive modes). Also, tested prototype version of coherent X-band radar.
    - Imaging footprints of the two radars are shown in Figure D1
    - Average radar image (WIMR) is shown in Figure D2 left panel illustrating inlet morphology.
    - Initial bathymetric estimation and wave direction vectors through the inlet are shown in Figure D2 right panel.
    - Inlet plumes are imaged in the WIMR lowpass filtered image sequences as shown in Figure D3. Back of the envelope estimate is that the ebb plume fronts were propagating at ~10 cm/s over a 2.5 hour period.
- Still awaiting delivery of the final version of the solid-state coherent X-band radar. To be delivered early in 2013.
- Published: Holman, R.A. and M.C. Haller, Nearshore remote sensing, *Annual Review of Marine Science*, to appear in Volume 5, January 2013.
- Under revision: Catalán, P.A., M.C. Haller, and W.J. Plant, Microwave backscattering from surf zone waves, *J. Geophys. Res.*, 2012.

Ongoing analysis involves:

1) Quality Control – WIMR complete, coherent-on-receive incomplete, fully coherent nearly complete.
2) Performing PIV analysis on plume fronts in lowpass filtered image sequences (in collaboration with Chickadel). Results will be compared with dye observations and numerical models.
3) Comparison of Doppler velocities (fully coherent system) with in-situ wave observations.
4) Adding more physics to the depth-inversion problem. Presently we have conducted depth-inversions without regard to the effects of currents (see Figure D2). Next steps are to incorporate the effects of currents and to quantify their effect on the inversion.
5) Collaborate with modelers on potential data assimilation schemes.

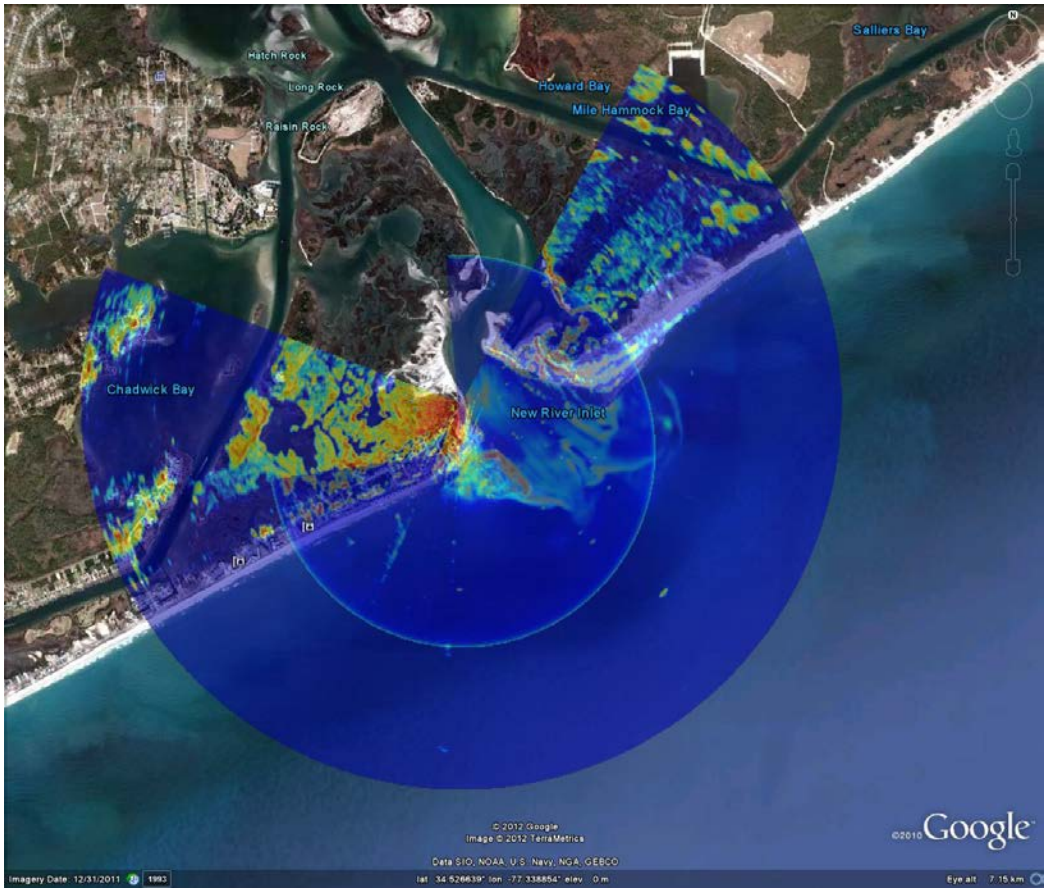

Figure D1: Example average radar images illustrating the imaging footprint at the New River Inlet site. Smaller circle is the image from the coherent system (installed at the house on beach), larger circle is from the WIMR installed on the scaffolding on the southwest side of the inlet.

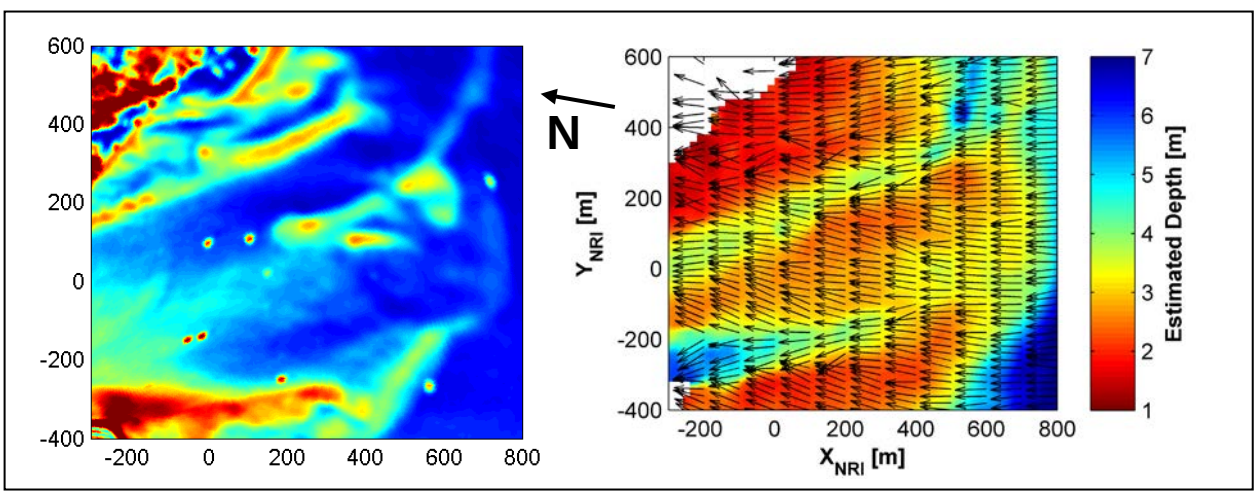

Figure D2: (left) Average radar image from WIMR. Greens, yellows, and reds are higher backscatter intensity due to wave breaking at low tide and illustrate the complicated inlet morphology, (right) bathymetry estimated via depth-inversion of the wave image sequences collected by WIMR. Wave direction vectors are shown as an overlay and demonstrate criss-crossing wave directions over the edges of the shoals.

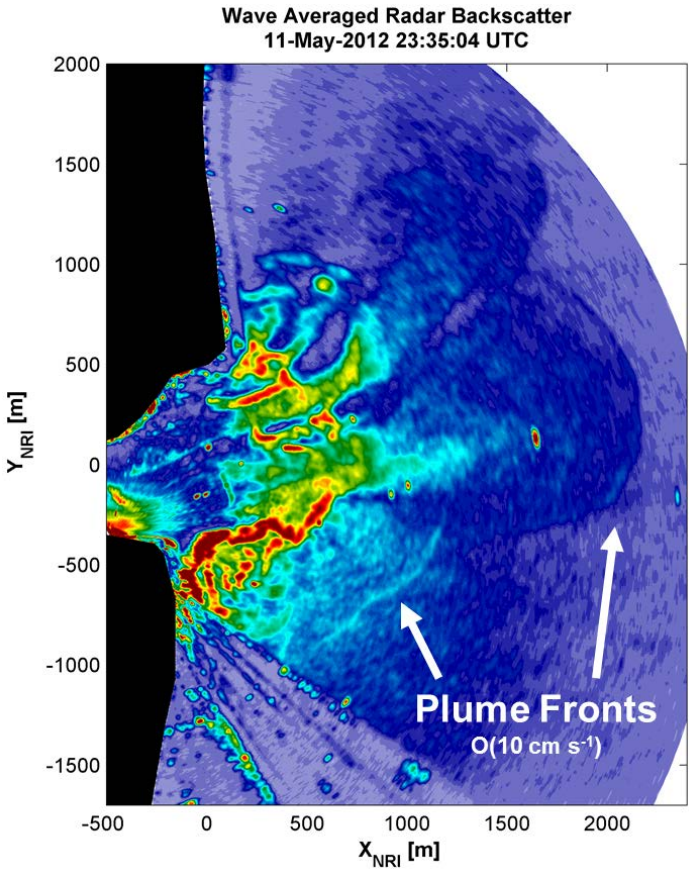

Figure D3: Single image from a WIMR lowpass filtered image sequence. Image shows plume fronts at x= 1km and 2km (see arrows). Red and yellow features are wave breaking over the inlet morphology. Qualitative estimates of the plume trajectories suggest propagation speeds of ~10 cm/sec.

D. In Situ Measurements – UW

The objective of the UW in situ measurements is to measure the properties and processes at the water surface that control remote sensing signatures, such that inversion for geophsical variables is improved. The approach is to measure surface turbulence in a wave-following reference frame using drifting SWIFT buoys (Surface Wave Instrument Floats with Tracking). A SWIFT schematic and example result is shown in Figure E1. The primary instrument onboard is an uplooking pulse-coherent Doppler sonar (2 MHz Aquadopp HR), which measures turbulence in a profile immediately beneath the surface (i.e., within 0.5 m). The second-order structure function of the turbulence is calculated and used to infer the turbulent energy dissipation rate, following Kolmogorov's theoretical energy cascade. The dissipation rate is associated with wave breaking, surface roughness, and wind drag, all of which affect remote sensing signatures. The SWIFTs also measure wave spectra, winds, and surface mean currents. In addition, two stationary meteorological stations and three tide gages were maintainted during the RIVET experiment.

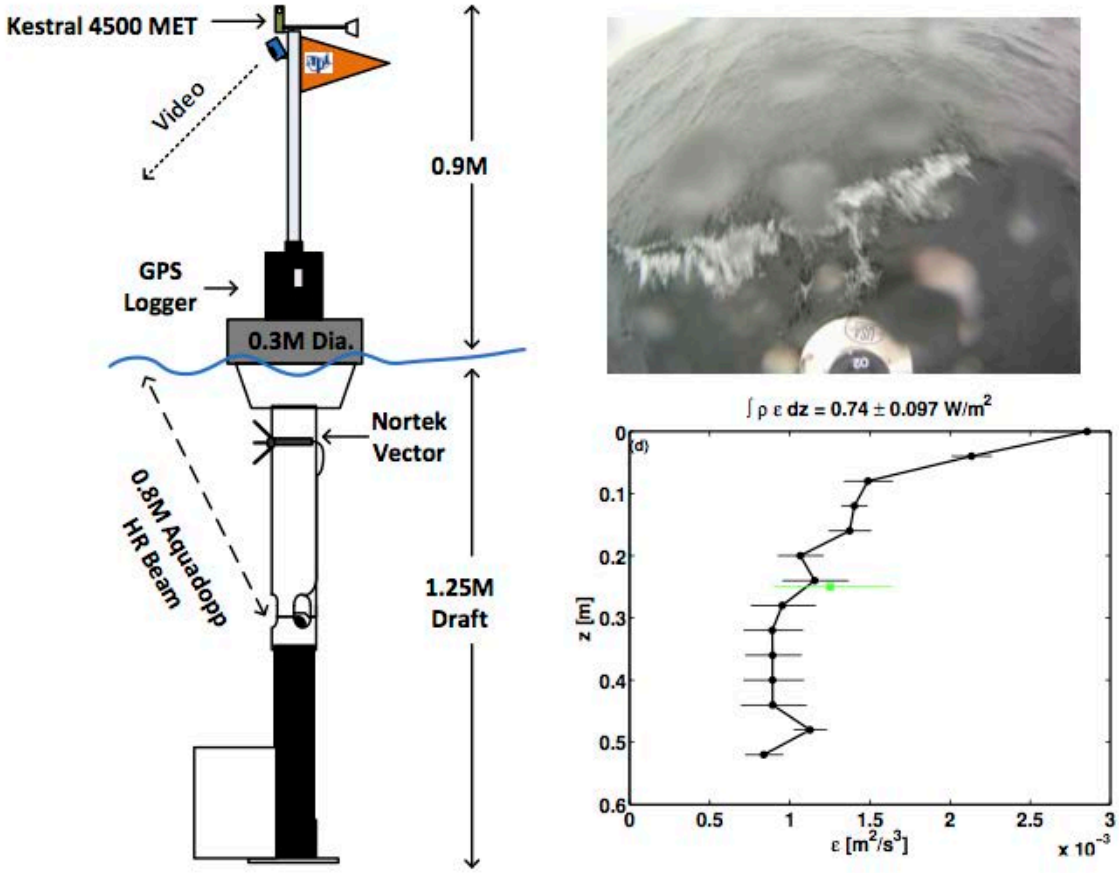

Figure E1. The Surface Wave Instrument Float with Tracking (SWIFT, left panels) and wave breaking example (right panels). The image of the breaking wave is taken from the mast of the SWIFT and the profile of dissipation rate ε(z) is calcualted from the turbulence measurements.

SWIFT data processing methods have been refined and accepted for publication. Much of this work used data collected from the Field Research Facility in Duck, NC in a previous year of this project. Four new SWIFTs have been fabricated and tested, resulting in a total of six operational SWIFTs.

The six SWIFTs were operated daily for one month during the RIVET experiment at New River Inlet. The operations were timed to coincide with airborne and tower-based remote sensing measurements. Sampling covered all tidal conditions and a range of wind-wave conditions. The resulting SWIFT tracks are shown in Figure E2.

The processed SWIFT data from New River Inlet show an expected pattern of enhanced dissipation over the shoals, where depth-limited wave breaking occures. The processed SWIFT data also show enhanced dissipation in the channels during ebb tides, consistent with steepness-limited wave breaking caused by an opposing currents. Finally, the processed SWIFT data show enhanced dissipation during strong winds. Preliminary analysis suggests that an energy budget can be prescribed using the surf parameter γ (= H/d = wave height over depth), the wave frequency shift ω (= u • k = tidal current times wavenumber), and the wind stress (= $C_D U^2$ = drag times wind speed squared). These parameters not only describe transfer of energy at the surface but they also quantify the mechanisms for surface roughness and thus remote signatures.

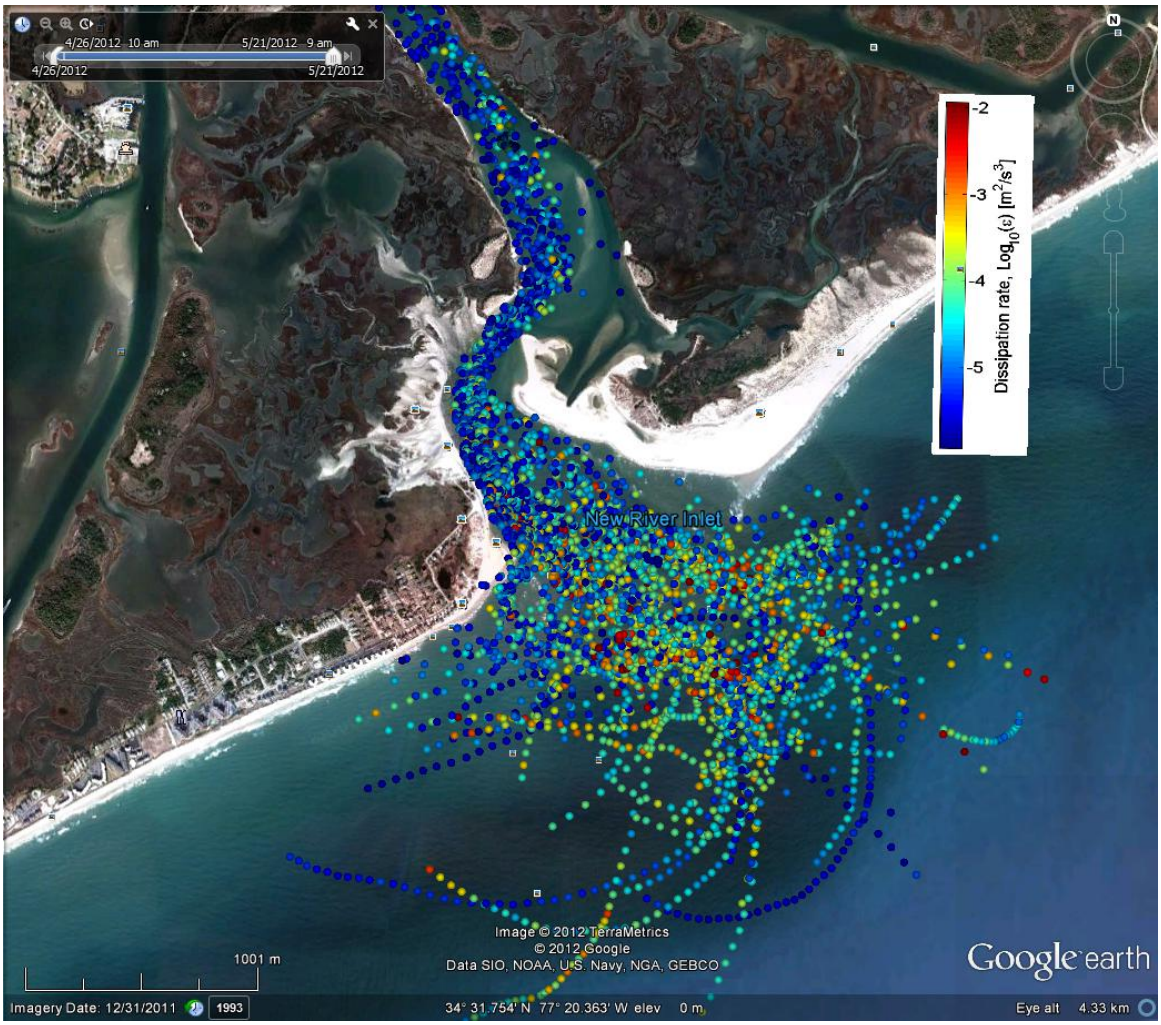

Figure E2. Aggregate SWIFT tracks from the month-long experiment at New River Inlet. Colors indicate surface dissipation rate (log scale).

F. In situ Measurements – WHOI

Waves and current sensors were deployed at 32 locations near New River Inlet from April 27 through June 1, 2012 (Figure F1). The data have undergone initial quality control and have been placed on the WWW for use by other ONR team members and colleagues. Analysis of the data has begun.

Analysis of the field observations from New River (Figure F1) began this summer. PhD student Julia Hopkins produced maps of mean flows for 846 one-hour data runs that show the strongest ebb currents occur near low tide. Flood flows are weaker than ebb flows, and occur at high tide. PhD student Anna Wargula has shown that offshore waves affect the subtidal (periods longer than 30 hrs) current fluctuations by increasing the flow into the inlet. Anna also has shown that a cross-shore momentum balance holds between bottom stresses from the current in the inlet mouth and radiation stresses from waves propagating between the seaward edge of the ebb shoal and the inlet mouth. Other processes (pressure gradients, wind stress, acceleration, nonlinear terms) are being investigated.

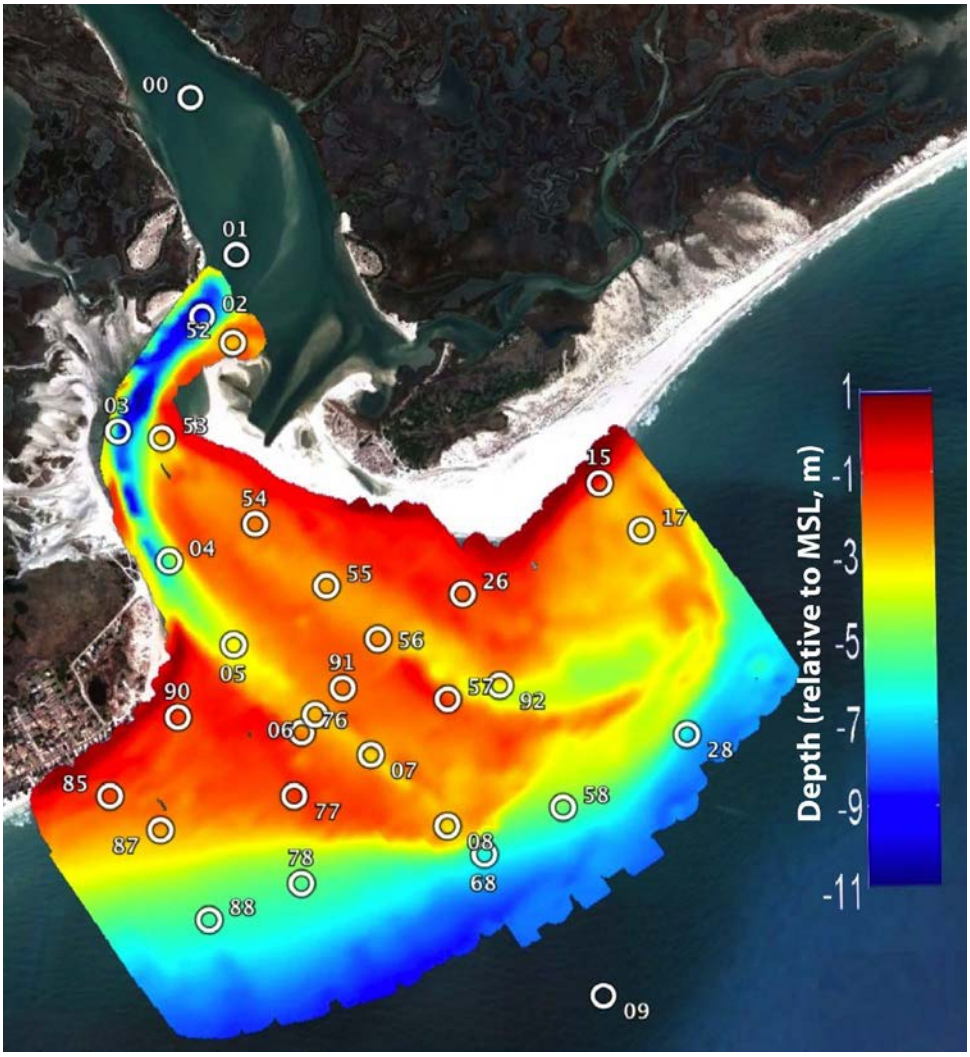

Figure F1. Array of in situ wave and current sensors (white circles) deployed at New River Inlet, spring 2012. The color contours are water depth (Provided by J. McNinch). [Instruments are located across the ebb shoal and about 2 km up the inlet channel in depths from 1 to 10 m].

G. Numerical Modeling and Data Assimilation – OSU

Our efforts have focused on a number of approaches. First, we have furthered our work on utilizing multiple observations types simultaneously to arrive at an estimate of the bathymetry. The data was assimilated (along with their confidence estimates) into a one-way coupled nearshore wave-circulation model to invert for bathymetry using ensemble methods and a least-square minimization concept. We have examined advantages derived from each data type, the time window of data needed for good convergence, and have quantified errors in the resulting bathymetry estimates. Second, we have been utilizing variational data assimilation techniques to build an adjoint to the one-way coupled wave and circulation model. The use of variational methods helps pinpoint the exact contribution made by the wave or circulation model components to the resulting correction in the bathymetry. Further, the required density and location of measurements can be explored. Third, we have been assembling a coupled wave-circulation model for the New River Inlet field site. Our modeling approach includes

nesting in larger scale wave forecasting and tidal models and our domain covers areas that reach far into the estuary. Finally, modeling efforts are underway for the simulation of the coupled wave-current field at the Mouth of the Columbia River. The preliminary results suggest area of influence of wave-current interaction processes and may be helpful in the design of the planned field operations.

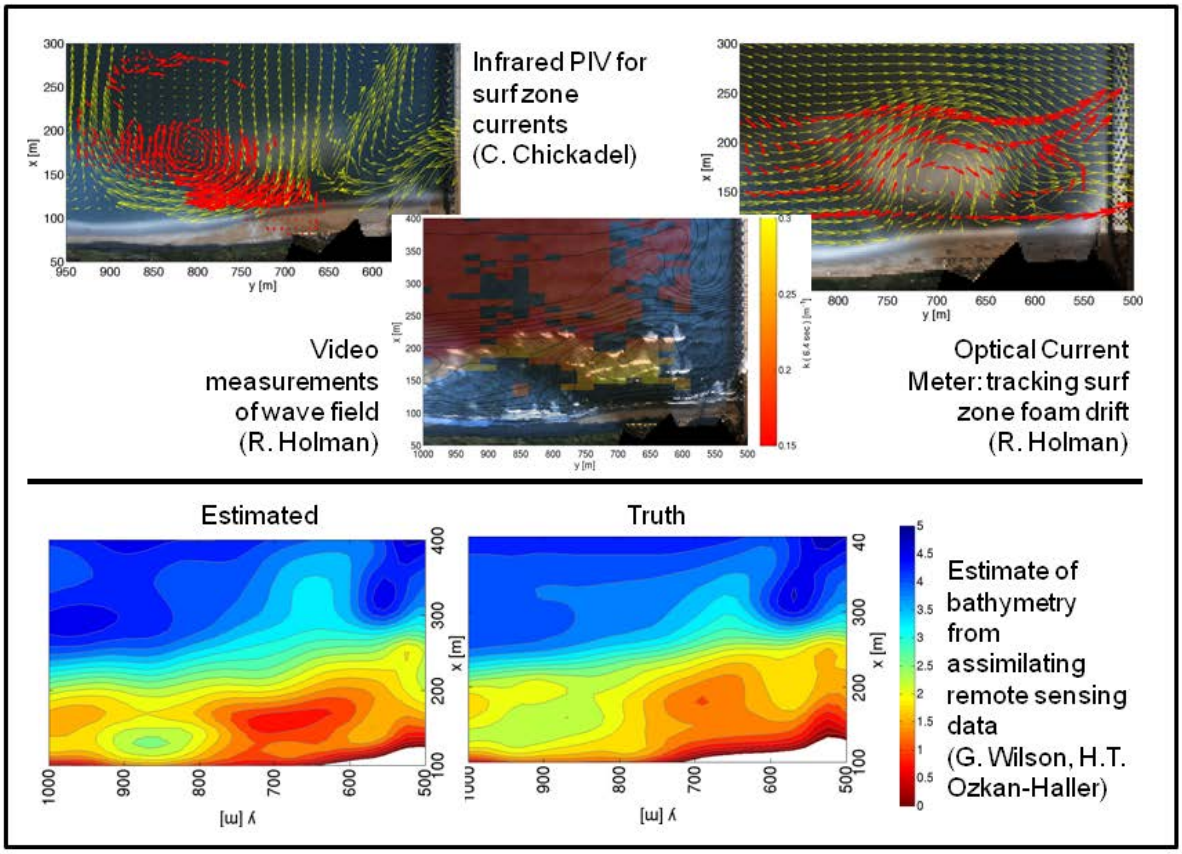

Figure G1: Several observations types (PIV from IR cameras, alongshore current observations from video cameras, wavenumber estimates from video cameras) were used alongside a one-way coupled wave-circulation model to produce estimates of bathymetry (given a prior guess that was based on the bathymetry 47 days earlier). The resulting bathymetry reproduces important features with a 30cm rms error.

Our work on using multiple observation types (see Figure G1) involved utilizing PIV current observations from IR cameras, observations of alongshore currents from video cameras, and observations of the wavelength at several frequency bands from video observations (such observations can also reliably be obtained from marine radars). The assimilation step resulted in estimates of bathymetry (see Figure G1) that were skilled (rms-error of 30 cm) and improved upon a prior guess (that was based on sampled bathymetry 47 days prior to the modeled conditions). Further, the assimilation step significantly improved the bathymetry estimate even after only assimilating one snapshot of observations (that were gathered using a 30 min collection window). The estimated bathymetry captured several important bathymetric features which had developed in the intervening days. For instance, the estimate captures a large shoal located at approximately y = 700 m; this shoal was responsible for much of the alongshore-nonuniform gyre-like flow observed in this time period,

hence was a very important feature dynamically. Similarly, a channel-like feature at approximately y = 850 m was also partly captured (note we have not assimilated observations for y > 900 m, hence the estimates are not strongly controlled there). And finally, the offshore region x > 250 m was made deeper by the assimilation of data, in agreement with the measured changes. These corrections resulted in an increase in bathymetric accuracy.

Additional experiments were performed to assess the importance of different data types on the results. We found that wavenumber data provided by far the most information, producing an accurate result after only one or two assimilation steps. Velocity data also produced accurate estimates of bathymetry, and reproduced the same qualitative bathymetric features, but the convergence to the result was relatively slow, and in the case of IR-PIV the corrections were limited by the field of view of the camera. The main reason for slow convergence when assimilating velocity data was that the data were sparse in space/time. This is because remote sensing-based estimates of velocity rely on tracking of visible features such as coherent structures or drifting foam. These features occur only occasionally, and can be ephemeral. By contrast, surface waves are almost always visible over a broad field of view, and provide information at multiple frequencies. As a result, there was an order of magnitude more data points for wavenumber than for velocities.

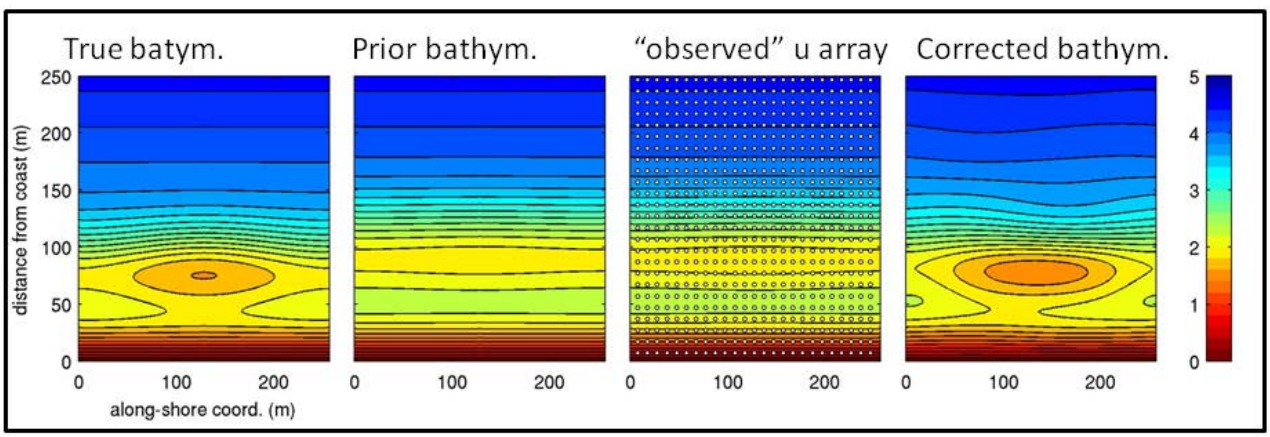

Figure G2: (from left) True bathymetry, prior guess bathymetry, prior guess bathymetry with observation locations, corrected bathymetry. The prior bathymetry lacks alongshore variability and has a bar at an incorrect cross-shore position. Assimilation of an array of velocity observations results in a correction of the bathymetry that involves introduction of alongshore variability and correction of the bar position.

Although the ensemble-based method is simple, useful and model-independent, it has several limitations. For example, there exists an implicit linearization about the prior estimate of bathymetry that we have attempted to overcome through the use of an iterative scheme. Although this approach is promising, it nonetheless adds significant cost in terms of computational needs. Also, results can be sensitive to whether or not the ensemble characterizes the variability in the system, and dependencies on multiple parameters may result in large ensembles. An elegant way to overcome these shortcomings involves the use of tangent linear and adjoint components of the coupled wave-circulation modeling system. This approach has given some very promising results during twin-experiments (when the model is sampled to generate synthetic data). In these experiments (see Figure G2), a true bathymetry is assembled that is characterized by a sandbar with significant alongshore variability. The prior guess bathymetry lacks this variability but does feature a sandbar, albeit at an incorrect cross-shore position.

Observations of velocities in an array of points similar to that produced by the optical current meters are assumed. Results reproduce the shift in bar location as well as the alongshore variability.

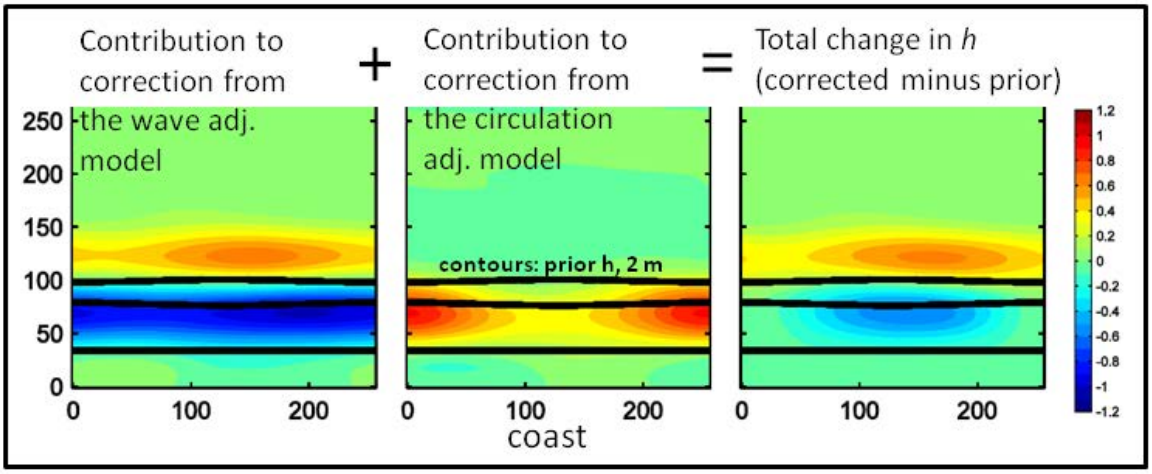

Figure G3: (from left to right) Contribution to the bathymetry correction by wave model, circulation model and both models The wave model provides correction the bar location without any alongshore variability, whereas the circulation model provides an alongshore variable correction without changing the bar location.

The variational data assimilation formalism now allows for the analysis of the correction step. In this case, we are interested in assessing the contribution of the wave model and circulation model to the correction in the bathymetry (see Figure G3). Surprisingly, we find that the wave and circulation models each are responsible for a different aspect of the correction. The wave model is primarily responsible for the determination of the correct bar location. Hence the correction due to the wave model is essentially alongshore uniform. In contrast, the correction due to the circulation model doesn't alter the cross-shore position of the bar, but introduces significant alongshore variation. The combination of the two corrections leads to the correct bathymetry. These results suggest that the two model components in essence contain unique information about the bathymetric state.

Finally, we are expanding on the coupled forecast modeling framework (SWAN+ROMS) that we had assembled for the conditions expected during the RIVET experiment at the New River Inlet in NC (see Figure G4). Of particular concern has been the utilization of wetting/drying effects in the estuary, the inclusion of coastal circulation features (e.g. forced by large scale pressure gradients) and inclusion of the upstream estuary. We are currently in the process of expanding the modeling domain so that a large part of the NC shelf is included. A nested smaller domain that includes the immediate inlet is then established. Comparison to surface elevation observations form the experiment shows that the circulation model has some immediate skill when compared to the tidal signatures in the estuary. Detailed data-model comparisons are the subject of further work.

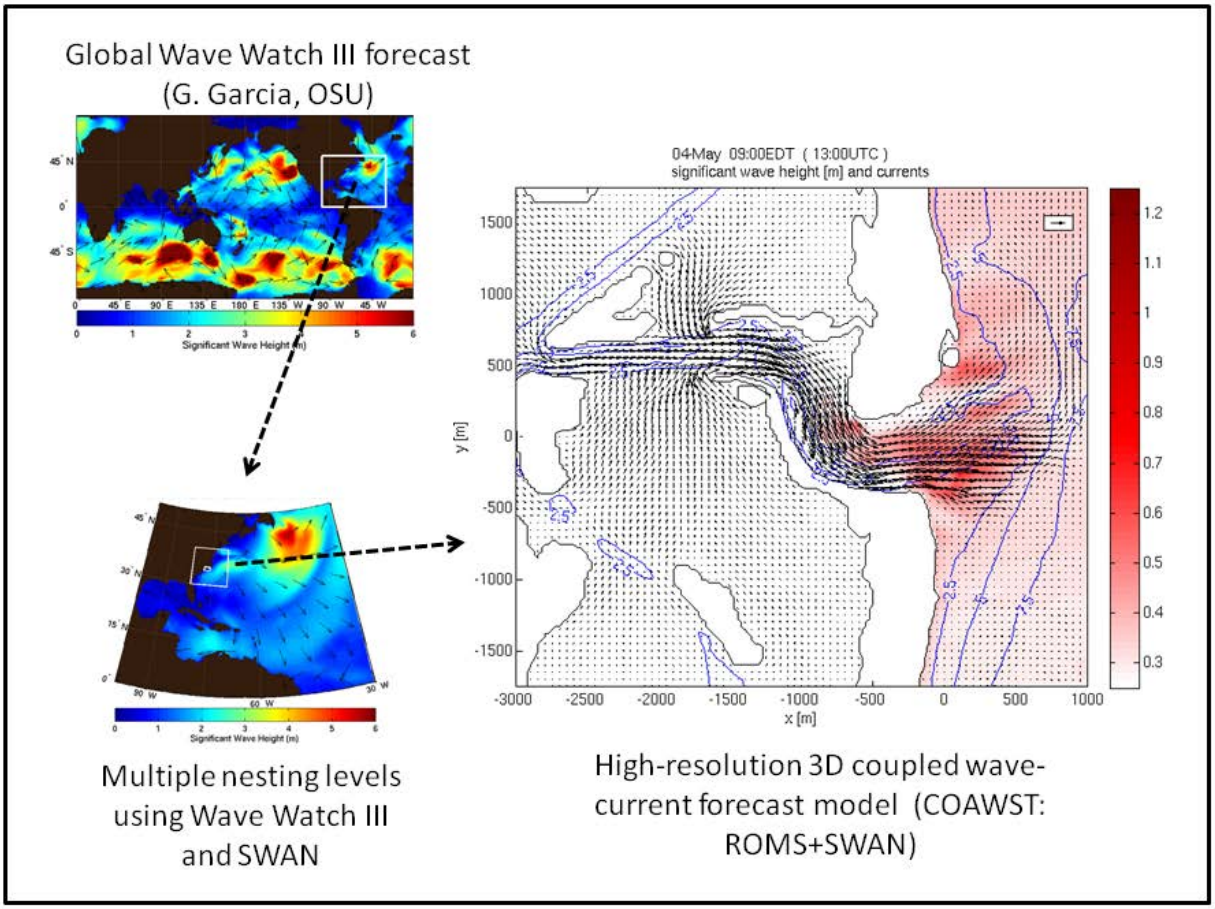

Figure G4: Nested model domains ranging from a global wave forecasting model (top left) to a regional domain (bottom left), to the local New River Inlet domain (right). During these mild wave conditions, wave amplification over the ebb currents is evident.

IMPACT/APPLICATIONS

Our results demonstrate how currently available prediction schemes and remote sensing observing systems can be combined for operational applications. Use of a miniaturized airborne along-track-interferometic SAR to measure surface velocities provides a new and powerful tool for area-extensive measurements in the field. The development of cBathy has high impact in finally allowing robust estimation of bathymetry with reasonable accuracy based only on continuing optical (or radar or IR) sampling. Bathymetry has always been an expensive and very rare variable to measure and one whose absence destroys the credibility of numerical model predictions.

RELATED PROJECTS

The DARLA MURI effort is closely related to the ongoing ONR RIVET DRI through participation in field campaigns. This work complements the traditional interests of NRL-SSC in littoral remote sensing including the LENS program and continuations thereof and efforts to carry out nearshore prediction based on UAV sensor inputs. This work also complements recent Oregon State efforts in which I am involved to greatly improve the utility and usability of UAV platforms for all purposes.

PUBLICATIONS

Catalán, P.A., M.C. Haller, and W.J. Plant, Microwave backscattering from surf zone waves, *J. Geophys. Res.*, 2012.

Holman, R.A. and M.C. Haller, Nearshore remote sensing, *Annual Review of Marine Science*, to appear in Volume 5, January 2013. [in press]

Holman, R.A., Plant, N.G. and K.T. Holland, cBathy: A robust algorithm for estimating nearshore bathymetry, *J. Geophys. Res*., 2012.

Thomson, J., Observations of wave breaking dissipation from a SWIFT drifter, *J. Atmos. & Ocean. Tech.*, 2012. [in press]